مجلة الدراسات التربوية والعلمية - كلية التربية - الجامعة العراقية
العدد الخامس والعشرون - المجلد الثالث عشر - علوم الكيمياء - آب 2025 م
doi.org/10.52866/esj.2023.13.25.27

Performance of Silver Nanoparticles Synthesized from *Sargassum boveanum* Leaves extract and Functionalized with Sulfurized Ligands for Mercury (II) Detection in Water

Asst.Lec. HADEEL JALAL ABBAS

Abstract :

The present study focuses on the synthesis and characterization of silver-cysteine (Cys-AgNPs) nanoparticles, utilizing natural reductants from the aqueous extract of *Sargassum boveanum*, with particle sizes under 100 nm. Transmission electron microscopy (TEM) analysis revealed that the Cys-AgNPs were spherical in shape, with an average particle size of 60 nm.

These Cys-AgNPs were then employed to detect mercury ions (Hg^{2+}) in environmental samples using the digital image technique as an alternative analytical tool. The combination of digital imaging and silver nanoparticles proved effective for the colorimetric analysis of mercury ions, yielding highly accurate results. In the absence of NaCl, Cys-AgNPs demonstrated a detection limit (LoD) of 5.79 ppb for Hg(II) ion analysis using the digital image method. When 0.5 M and 1 M NaCl were added, the LoD values improved to 2.46 ppb and 3.02 ppb, respectively.

The accuracy of the digital image method was found to be over 99% when compared to UV-Vis spectrophotometry, highlighting that the digital image method provides superior accuracy in the quantitative analysis of heavy metals such as Hg(II) using AgNPs, when compared to conventional UV-Vis spectrophotometric techniques.

Keywords: *Sargassum boveanum* aqueous extract, silver-cysteine nanoparticles, characterization, Hg(II) ion analysis.

أداء جسيمات الفضة النانوية المُصنَّعة من مستخلص أوراق Sargassum boveanum ووظيفتها باستخدام الروابط الكبريتية للكشف عن الزئبق (II) في الماء

م.م هديل جلال عباس

مستخلص:

تركز الدراسة الحالية على تخليق وتوصيف جسيمات الفضة والسيستين (Cys-AgNPs) النانوية، باستخدام مواد اختزال طبيعية من المستخلص المائي لنبات Sargassum boveanum، بأحجام جسيمات أقل من 100 نانومتر. كشف تحليل المجهر الإلكتروني للإرسال (TEM) أن Cys-AgNPs كانت كروية الشكل، بمتوسط حجم جسيم يبلغ 60 نانومتر.

تم بعد ذلك استخدام Cys-AgNPs للكشف عن أيونات الزئبق (Hg^{+2}) في العينات البيئية باستخدام تقنية الصورة الرقمية كأداة تحليلية بديلة. أثبت الجمع بين التصوير الرقمي والجسيمات النانوية الفضية فعاليته في التحليل اللوني لأيونات الزئبق، مما أدى إلى نتائج دقيقة للغاية. في غياب كلوريد الصوديوم، أظهرت Cys-Ag-NPs حد اكتشاف (LoD) قدره 5.79 جزء في البليون لتحليل أيون الزئبق (II) باستخدام طريقة الصورة الرقمية. عند إضافة M0.5 و 1M .

تم العثور على دقة طريقة الصورة الرقمية بأكثر من 99٪ بالمقارنة مع القياس الطيفي للأشعة فوق البنفسجية المرئية، مما يسلط الضوء على أن طريقة الصورة الرقمية توفر دقة فائقة في التحليل الكمي للمعادن الثقيلة مثل الزئبق (II) باستخدام AgNPs، عند مقارنتها بتقنيات قياس الطيف الضوئي التقليدية للأشعة فوق البنفسجية.

الكلمات المفتاحية: المستخلص المائي Sargassum boveanum، جزيئات الفضة والسيستين النانوية، التوصيف، تحليل أيون الزئبق (II).

1. Introduction

Electrochemical techniques have sparked significant interest in the search for new alternatives due to their ease of use, short analysis times, simplicity, and ability to determine the oxidation state of the element(s) of interest individually or concurrently with small sample volumes [1]. However, as electrochemical techniques advance, it becomes clear that the composition of the working electrode is an important factor. Carbonaceous or metallic elements such as Ag, Au, and Pt are commonly used in conventional electrodes, which have low sensitivity and selectivity. Metallic nanoparticles can overcome this disadvantage [2]. In this context, green chemistry provides a new perspective on the future of nanomaterials by producing nanoparticles (NPs) from natural and non-toxic organic sources such as plants, fruits, herbs, and fungi using a simple, scalable, and non-toxic process. Solvents and reducing agents enable the production of metallic nanostructures coated with an organic film that inherits some properties of the active compounds of the source used [3], providing them with additional functionality, as demonstrated for other nanostructures. In addition, they have a significant impact on the morphology of the synthesized particles, such as their size and physicochemical properties, allowing for green synthesis. Following synthesis, NPs can be coated with the desired molecules to facilitate chemical interaction [4].

Mercury (Hg) concentrations in the environment have risen dramatically in recent years. Mercury is a volatile element, and Mercury (II) ions (Hg(II)) dissolved in water [5] are one of the most common and stable forms of mercury pollution. Mercury can harm the brain, liver, kidneys, lungs, and immune system in humans [6], and given the risks to human health, research is needed to develop an easy, cheap, sensitive, and accurate method for detecting Mercury. Previous research [7-8] demonstrated that mercury can be detected with silver nanoparticles (AgNPs). This is due to AgNPs' optical sensor properties, which can be used as a colorimetric indicator to detect Hg (II) ions [6]. However, the sensitivity of AgNPs as a Hg (II) ion detector remains low [7]. Sulistiawaty et al.'s (2015) [9] study on the sensitivity of

AgNPs as a Hg (II) ion detector using the UV-Vis spectrophotometry method yielded a Limit of Detection (LoD) of 0.13 ppm [8], but the resulting LoD value was insufficient to detect Hg (II) ions up to a concentration of 5 ppb, which is the maximum limit of Mercury concentration allowed to be contained in water in the environment [9]. Because of their low sensitivity, AgNPs require a new method for increasing their sensitivity as a detector of Hg (II) ions. AgNP-based calorimetric methods have been widely used to rapidly detect a variety of analytes, including organic molecules, toxins, drugs, and metal ions, because they do not necessitate complicated or lengthy protocols and overcome some of the limitations of traditional methods. The optical properties of AgNPs are largely determined by the size, shape, and aggregation of NPs in solution, which are controlled by the LSPR [10]. AgNP-based colorimetric sensors for Hg(II) detection can use one of two detection mechanisms: a redox reaction of AgNPs with Hg(II), which causes a variation in the LSPR intensity and/or a shift in the AgNPs extinction wavelength between 390-410 nm due to the formation of a nanoalloy (Ag-Hg); or an aggregation process of AgNPs with Hg(II), which acts as a bridge between AgNPs. This last process reduces LSPR and creates a new band between 500 and 650 nm [11]. Both mechanisms cause a colour change in the solution, and as a result, the extinction of the LSPR band decreases, establishing a link between the extinction value of AgNPs and mercury concentration (II). The standard electrode potential of Ag+/Ag (0.80 V) is lower than that of Hg(II)/Hg (0.85 V), allowing Hg(II) to react with AgNPs to form metallic mercury [12]. Following that, the silver nano amalgam (nanoalloy) is formed. Hg(II) alters the surface of AgNPs, causing a change in the zeta potential and destabilizing the colloidal system. AgNP aggregation by Hg(II) is controlled by the nature of molecules and ligands present on the particles' surface; due to the affinity and selectivity of the functional groups on them, the specific molecular recognition of ligands by metal ions acts as a bridge connecting the AgNPs [13].

In this study, an aqueous extract of *Sargassum boveanum* (commonly known as cattle sargassum), a seaweed from the Sargassaceae family in

the plant kingdom [14], was used due to its high concentration of phenolic compounds (such as phenolic acids and flavonoids) and total reducing sugars. This chemical composition imparts *Sargassum boveanum* with strong antioxidant properties [15], making it an ideal candidate for the synthesis of silver nanoparticles (AgNPs) with an organic coating rich in functional compounds and groups [16].

AgNPs were chosen for their unique physicochemical properties, including an excellent surface-to-volume ratio, optoelectronic characteristics that vary with shape and size, high biocompatibility, and very low toxicity. These qualities make AgNPs highly promising for applications in biomedicine, catalysis, and photonics.

This study aimed to develop an accurate and sensitive method for detecting Hg(II) ions using digital image analysis combined with AgNPs as a colorimetric sensor. This approach is expected to enable the detection of Hg(II) ions at low concentrations, offering a reliable and efficient analytical tool for environmental and health monitoring.

2. Materials and Methods

The chemicals, $AgNO_3$, NaCL, $HgCl_2$, L-cysteine used in this study were sourced from Sigma-Aldrich (USA), Merck, and SD Fine Chemicals, all of which were of 98-99% analytical reagent (AR) grade purity. Ultrapure double-distilled water was used throughout the study to ensure the highest quality and accuracy in all experiments.

2.1 Preparation of *Sargassum boveanum* extract

The *Sargassum boveanum* extract was prepared using an infusion method. Using a household blender, the Sargassum biomass was ground into a fine powder (40 mesh). Two grams of the *Sargassum* powder were mixed with 100 mL of distilled water, and the mixture was homogenized by magnetic stirring (Remi-2L model shaker) at 80°C for 90 minutes. Afterward, the mixture was allowed to cool to room temperature. The liquid phase was separated by filtration using Whatman 41 filter paper. The resulting extract was stored in an amber vial at 4°C until further use.

For the synthesis of silver nanoparticles (AgNPs), the precursor solution

(0.2 M AgNO3) was mixed with the prepared *Sargassum* extract, as shown in Figure 1.

2.2 Biosynthesis of Silver Nanoparticles(AgNPs)

The biosynthesis of AgNPs is carried out by mixing *Sargassum boveanum* extract with a 1 mM $AgNO_3$ stock solution in a 1:9 ratio and stirring the mixture for 15 minutes using a magnetic stirrer. The mixture is then exposed to sunlight for varying durations of 15, 30, 45, and 60 minutes to induce the formation of AgNPs [17].

After determining the optimum heating time, each AgNP solution is stored for 1, 2, and 7 days, respectively. The formation of AgNPs is visually observed, and their characteristics are analyzed using a UV-Vis spectrophotometer, with measurements taken across the wavelength range of 280 to 700 nm. The pH of each AgNP solution is also recorded.

The wavelength that produces the maximum absorbance in the 400 to 500 nm range is identified as the characteristic wavelength for AgNP formation. The corresponding formation time is selected as the optimum time for synthesizing AgNPs based on the maximum absorbance observed.

2.3 Synthesis of Cys-AgNPs

To stabilize the AgNPs with an affinity for Hg (II), this research employed small molecules containing sulphur groups (thiols), such as cysteamine and cysteine, as stabilizing agents [18]. Silver-cysteine nanocomposites (Cys-AgNPs) were synthesized using a previously reported method with slight modifications.

The process was as follows:

a. Two concentrations of L-cysteine were tested, specifically 0.01 M and 0.001 M.

b. First, 100 mL of a 0.001 M AgNO3 solution was prepared in a 250 mL Erlenmeyer flask, which was then stirred at a constant speed of 250 rpm at room temperature.

c. Next, 1 mg of *Sargassum boveanum* extract was added to the $AgNO_3$ solution. The solution turned light yellow, indicating the formation of silver nanoparticles.

d. After 10 minutes, 2 mL of L-cysteine was introduced to the AgNPs solution, resulting in a colour change to deep yellow, signaling the formation of Cys-AgNPs.

e. The resulting Cys-AgNPs solution was stored at 5°C in a refrigerator to maintain the stability of the nanoparticles for further experiments.

2.4 Characterization of AgNPs:

The formation of Cys-AgNPs and the stability of the nanoparticles can be confirmed by monitoring the absorption intensity of the localized surface plasmon resonance (LSPR) band in the wavelength range of 300-700 nm using a UV-Vis spectrophotometer (Elico-SL 159). Additionally, the particle size of the Cys-AgNPs was analyzed using transmission electron microscopy (TEM) (JEOL-JEM-2100).

2.5 Determination of Cys-AgNP Sensitivity as an Hg(II) Ion Detector

To colorimetrically detect mercury ions (Hg^{2+}) using AgNPs, 1 mL of a standard solution containing Hg(II) ions at concentrations of 0, 0.1, 1, 10, 20, 25, 50, and 100 ppm was pipetted into individual 10 mL vials. Next, 2 mL of AgNP solution was added to each vial, and the colour changes that occurred over a 15-minute period were observed. Afterward, the solution was transferred into a cuvette and characterized using a UV-Vis spectrophotometer, with measurements taken across the wavelength range of 280 to 700 nm.

2.6 Increasing the Sensitivity of Cys-AgNPs as a Detector of Hg(II) ions

Increasing the sensitivity of Cys-AgNPs as a detector of Hg(II) ions was done by adding 0.5 and 1 M NaCl solutions into the Cys-AgNPs solution with a ratio of 1:5. Furthermore, the mixture was stirred for 15 minutes with a magnetic stirrer. Each Cys-AgNPs solution obtained was then put into a cuvette and characterized by a UV-Vis spectrophotometer using a wavelength of 280 to 700nm.

2.7 Image Capture and Calibration Curve Creation for Digital Image Method:

- Blank solution is prepared in the form of distilled water and a mixture of Cys-AgNPs + Hg(II) ions with Hg(II) ion concentrations of 5, 10, 15, 20, 25 ppb, respectively
- Next, the blank solution and the mixture of Cys-AgNPs + Hg(II) ions with various concentrations that have been prepared are placed in a mini studio and photographed with a Xiomi X4 cellphone camera.
- The image is then processed using MATLAB R2010b to obtain the RGB

component value.

• The absorption intensity value (A) of each RGB colour component is calculated using Microsoft Excel 2019 with equation 1.

$$A = \log\left(\frac{I_0}{I_t}\right) \quad Eq.(1)$$

Where:

A = Intensity of colour component absorption

I_0 = Value of blank solution colour component

I_t = Value of standard solution colour component

Then, from the absorbance results obtained, a standard curve (calibration) of absorbance vs Hg(II) concentration was determined by using the simple linear regression (SLR) analysis technique [19].

3. RESULTS AND DISCUSSION

3.1 Synthesis and characterisation of Cys-AgNPs

The biosynthesis process of silver nanoparticles (AgNPs) using *S. bovea-num* aqueous extract is seen marked by a change in the colour of the solution to brownish yellow (Figure 1), with the pH value of the solution during the biosynthesis process will be around 5. In addition to changes in the colour of the solution, the results of the UV-Vis absorption spectrum are one of the characteristics that can be used to confirm the formation of AgNPs. The Localized Surface Plasmon Resonance (LSPR) value of AgNPs has a peak (417nm) in the range of λ_{max} 400-500 nm [20].

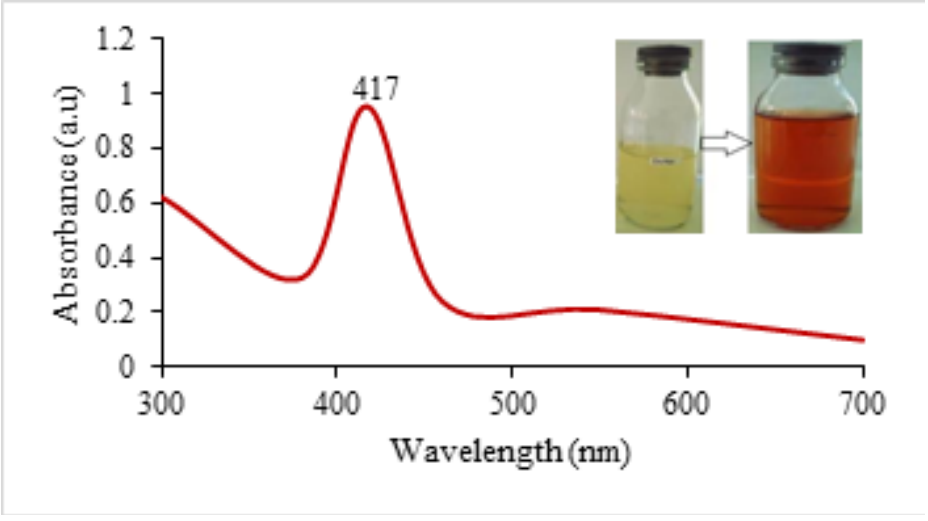

Figure 1: UV-Visible spectra of AgNPs from *S. bovea-num* aqueous extract and silver nanoparticles (AgNPs) formed (in the inset)

Because *S. boveanum* aqueous extract contains reducing agents like polyphenolic compounds, biosynthesis of AgNPs using this extract is possible [20]. Because polyphenolics have a standard reduction potential of +0.40 V < the standard reduction potential of Ag+ ions, which is +0.80 V, they function as a bioreactor. When polyphenolics donate electrons, they act as a reductant, and when Ag+ ions capture electrons, they act as an oxidant. The estimated amount of AgNPs formed is shown by the absorbance value derived from the UV-Vis spectrophotometry spectrum results. On the other hand, the size distribution of the resultant nanoparticles can be seen in the maximum wavelength spectrum (λmax). To more precisely ascertain the size, dispersion, and shape of AgNPs, additional TEM characterization is necessary. *S. boveanum* aqueous extract was used as a reducer in the room-temperature synthesis of Cys-AgNPs nanoparticles. One benefit of the chosen AgNP synthesis method is its ease of use, speed, and room temperature synthesis. A brownish-yellow hue was produced by the successfully synthesised Cys-AgNPs nanoparticles (Figure 1 inset). There was a slight colour difference between Cys-AgNPs at different L-cysteine concentrations. Nanoparticles with a slightly more concentrated colour were produced using 0.01 M L-cysteine (Figure 1 inset) as opposed to 0.001 M L-cysteine. The outcomes are different from those of the Prosposito et al. (2020) study [21], which found that the colour generated tended to be intense yellow. It is believed that the synthesis process was not conducted in a vacuum, which is why the colour difference was created. Nevertheless, the brownish-yellow hue remains one of the silver nanoparticles' properties.

Cys-AgNPs' UV-Vis spectrum from two distinct L-cysteine concentrations revealed an LSPR absorbance peak between 400 and 417 nm (Figure 2). Indicating that the cys-AgNPs treated with 0.01 M L-cysteine had superior nanoparticles, the 0.01 M L-cysteine treatment peak was narrower and higher than the 0.001 M L-cysteine peak. The plasmon peaks in both treatments were unstable, according to the findings of the nanoparticle stability test. Along with the duration of the nanoparticles' storage, Figure 2a showed a decrease, widening, and shifting of the peak to

the right. Along with the peak's decline, Figure 2b also showed the formation of a second plasmon peak in the 60 nm range, suggesting that some nanoparticles aggregated to form particles. It is necessary to store stable nanoparticles for an extended period of time. On the other hand, aggregable nanoparticles can be used for colorimetric biomolecular compound detection.

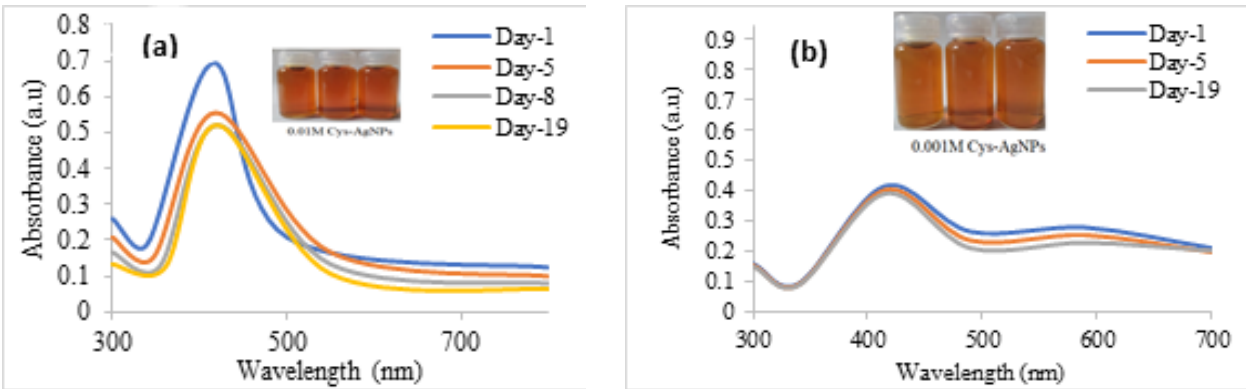

Figure 2: (a) UV-Vis spectra of Cys-AgNPs at 1, 5, 8, 19 days storage with 0.01M cystine concentration and (b) UV-Vis spectra of Cys-AgNPs at 1, 5, 19 days storage with 0.001M cystine concentration

The stability of Cys-AgNPs was also observed by looking at the UV-Vis spectra after storage. Figure 2 shows the UV-Vis spectra of a Cys-AgNPs colloid sample (0.01 M cysteine) that has been stored for 19 months at 4°C, which is still brownish yellow with a plasmon peak at 416 nm. Although the peak shifts slightly to the right, from 402 to 416 nm, it is still within the range of the plasmon peak for AgNPs, which is 390-450.

Figure 3:
TEM image with histograms of (a) Cys-AgNPs (b) Cys-AgNPs 0.5 M NaCl (c) 1M Na-Cl+Cys-AgNPs

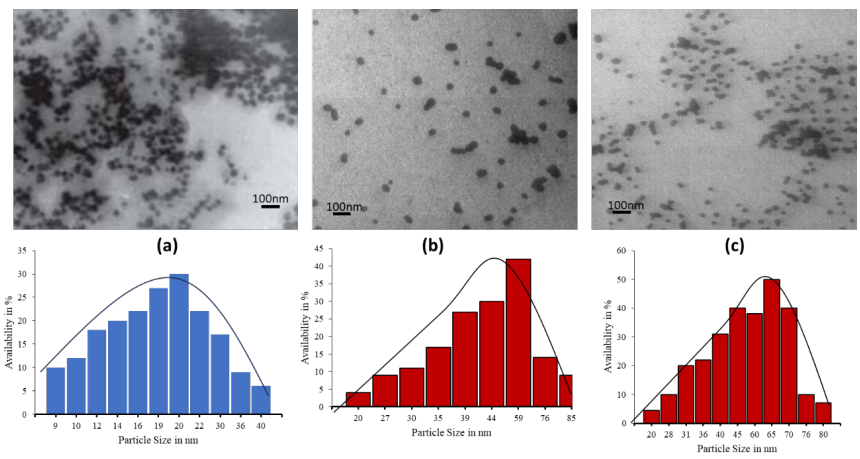

Figure 3 shows the TEM image and size distribution histogram of (a) Cys-AgNPs, (b) 0.5 M Cys-AgNPs NaCl, and (c) 1M NaCl+Cys-AgNPs. Figure 3a shows green synthesized silver nanoparticles with a 20nm size and cysteine-modified silver nanoparticles with a concentration of 1M have a particle size of 65 nm, whereas 60 nm particle size observed in 0.5M NaCl.

3.2 Determination of Cys-AgNPs Sensitivity as a Detector of Hg(II) Ions

It has been established that Cys-AgNPs can detect Hg(II) ions colorimetrically [22]. In a redox reaction, Cys-AgNPs will be oxidised by Hg(II) ions, converting its Ag0 atoms into Ag+ ions, when it is added to a mercury solution. The reduction potential of Hg(II)+0.92 V is higher than that of Ag+ ions, which is +0.80 V, which is what causes this oxidation process [22]. According to the study's findings, the more Hg(II) ions added to the Cys-AgNPs solution, the more Hg(II) ions will oxidise Cys-AgNPs, causing the solution to fade and even turn clear. This is illustrated in Figure 4.

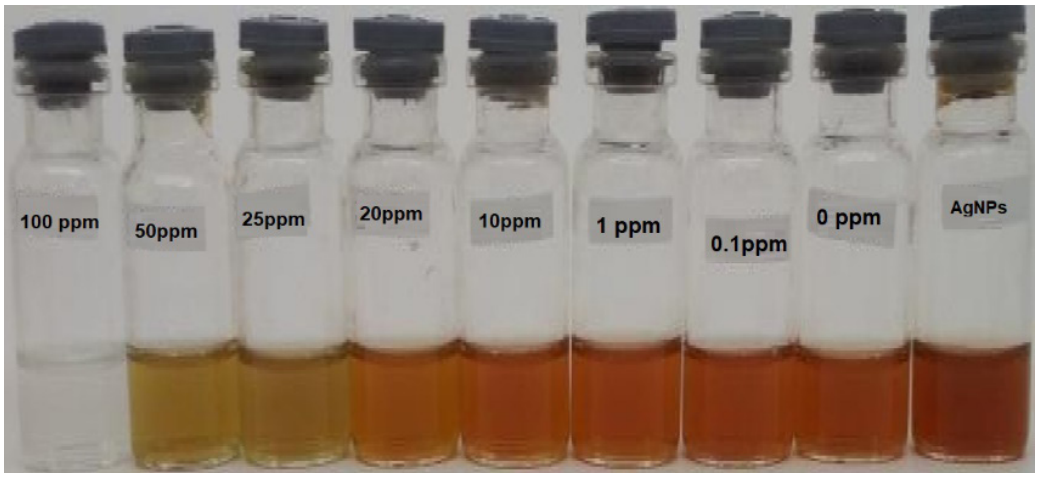

Figure 4. Results of visual observation of Cys-AgNPs from various concentrations of Hg(II) (100 -0 ppm)

Visual observation shows that at a concentration of 20-100 ppm, there has been a colour change from brownish-yellow to orange-yellow and yellow to clear. However, for a concentration of 2 ppb - 10 ppm, there was no significant colour change. Therefore, it is necessary to measure the absorbance

using UV-Vis spectrophotometry to see the difference in the absorption spectrum at each additional concentration of Hg(II) into Cys-AgNPs as seen in Figure 5.

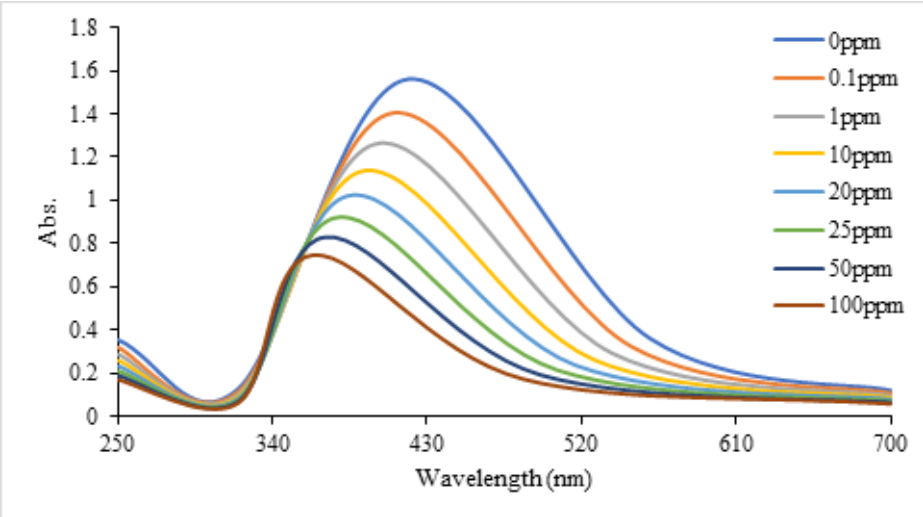

Figure 5. Cys-AgNPs spectrum after reacting with Hg(II) (0-100 ppm)

In Figure 5, the absorbance of Cys-AgNPs in Hg(II) solution at a concentration of 0.1 to 10 ppm tends to decrease with increasing concentration of Mercury ions in the solution and is accompanied by a slight shift in the λmax value. The decrease in absorbance and λmax values that are not too large indicates that the size and amount of Cys-AgNPs in the solution do not change too much so that the colour of the solution tends to be the same as Cys-AgNPs before being reacted.

When the colour of the reacted Cys-AgNPs solution becomes orange yellow (at Hg(II) 20 ppm), yellow (at Hg(II) 25 and 50 ppm), the absorbance tends to be low and λmax shifts significantly, and when the colour of the solution becomes clear, the Cys-AgNPs absorbance tends to widen significantly to flat, indicating that there is no Cys-AgNPs in the solution because it is suspected that Cys-AgNPs (Ag0) has been oxidized to Ag+.

3.3 Increasing the Sensitivity of Cys-AgNPs as a Detector of Hg(II) Ions

Inorganic salt compounds are added to increase the sensitivity. Because anions can alter the chemical characteristics of the nanoparticle surface,

Cys-AgNPs can be modified by NaCl and other inorganic substances [23]. A typical concentration of NaCl that can be applied to nanoparticles in the range of 0.01-3.0 mM can be reduced in size by the presence of NaCl ions [24]. According to Naganthran et al (2022) [30] research, the particle size will decrease with increasing NaCl concentration. The surface area of small Cys-AgNPs will be greater. Figures 6 and 7 show the impact of adding NaCl to Cys-AgNPs.

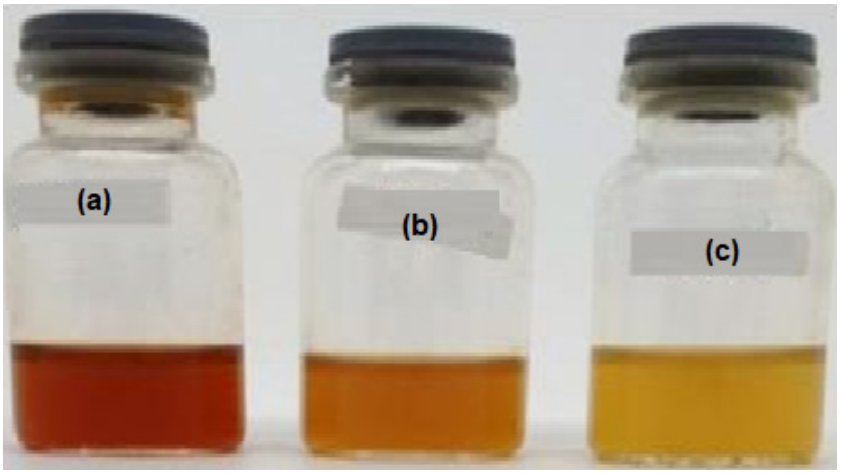

Figure 6.
Results of visual observation with the addition of NaCl (a) Cys-AgNPs (b) 0.5 M Cys-AgNPs NaCl (c) 1 M NaCl+Cys-AgNPs

From Figure 6, it can be seen that the addition of NaCl salt causes a change in the colour of Cys-AgNPs to a duller brownish yellow, to bright yellow. Figure 7 shows that adding NaCl causes a decrease in absorbance and a shift in λ_{max} towards a smaller wavelength. The greater the concentration added to Cys-AgNPs, the more λ_{max} shifts towards a smaller wavelength and the lower the absorbance.

According to De Leersnyder et al (2019) [25], the size of silver nanoparticles can be determined from the maximum absorption peak wavelength, where the larger the particle size, the more the absorption peak will shift towards a larger wavelength, and the wider peak formed [27]. Therefore, based on this explanation, the size of Cys-AgNPs will become smaller with the addition of NaCl, where the absorption peak at λmax will shift towards a smaller wavelength.

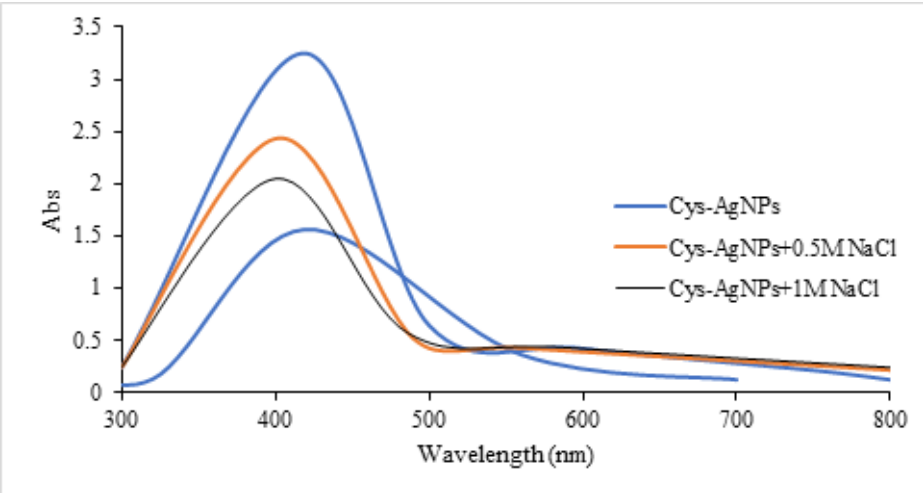

Figure 7. Cys-AgNPs spectrum resulting from the addition of 0.5 M and 1 M NaCl solutions

In addition, the decrease in absorbance when NaCl is added is caused by the presence of Cl- anions, so the energy on the surface of the nanoparticles easily changes, known as the effect of energy hybridization on the surface of the nanoparticles. Therefore, the absorbance spectrum can decrease drastically by the presence of anions [26]. This is what makes Cys-AgNPs unstable when NaCl is added. Meanwhile, the pH value of the solution during the process of adding NaCl to Cys-AgNPs is at pH 5. Adding NaCl to Cys-AgNPs has the same pH as the pH of Cys-AgNPs synthesis, which means that adding NaCl to Cys-AgNPs does not change the pH of Cys-AgNPs. The sensitivity of Cys-AgNPs added with NaCl to mercury ions (Hg(II)) can be seen in Figures 8 and 9. From Figures 8 and 9, it can be seen that the addition of NaCl to the Cys-AgNPs solution can increase the sensitivity of Cys-AgNPs in detecting Mercury ions. This is evidenced by the change in the colour of the solution to clear at a concentration of Hg(II) 25 - 100 ppm (Figure 8) and at a concentration of Hg(II) 20 - 100 ppm (Figure 9) compared to Cys-AgNPs without the addition of NaCl.

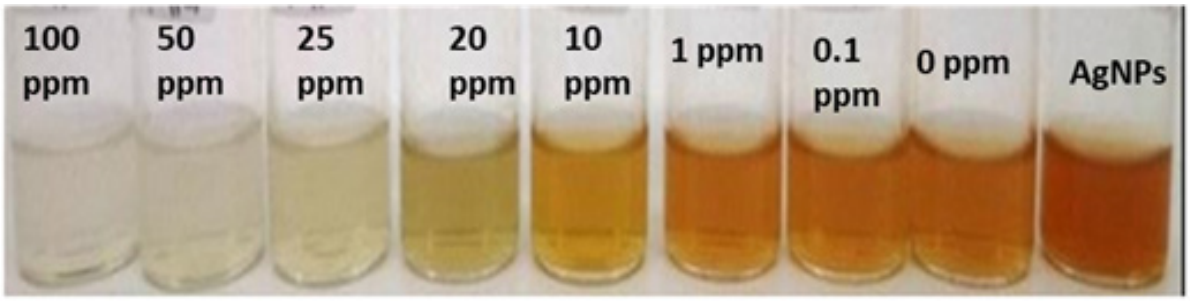

Figure 8. Results of Visual Observation of Cys-AgNPs (0.5 M NaCl) on Hg (II) solution (100 ppm-0 ppm)

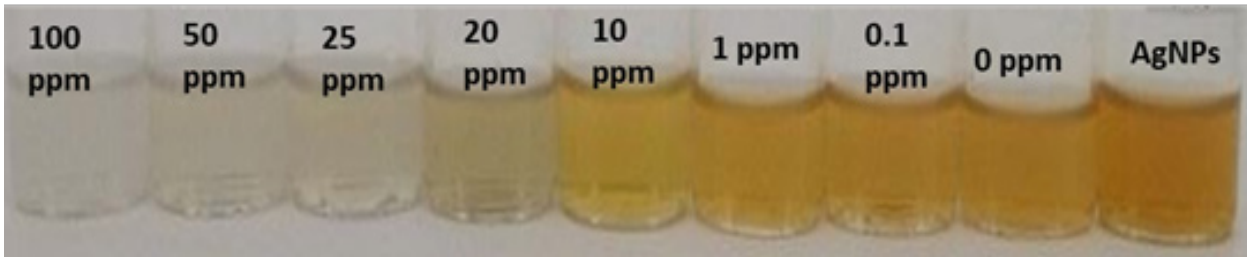

Figure 9. Results of Visual Observation of Cys-AgNPs (1M NaCl) on Hg (II) solution (100 ppm-0 ppm)

This increase in sensitivity may be due to the particle size of Cys-AgNPs with the addition of NaCl being smaller than the size of Cys-AgNPs without the addition of NaCl so that the smaller size of Cys-AgNPs will allow Cys-AgNPs to react more easily with Hg(II) ions.

There is a difference in sensitivity between the addition of 0.5 M NaCl and 1 M NaCl, where the greater the concentration of NaCl added, the more sensitive the Cys-AgNPs obtained will be to Hg(II) ions because the smaller the size of the Cys-AgNPs produced to react with Hg(II) ions.

3.4 Use of Digital Image Method in Hg(II) Ion Analysis

Because the digital image method is known to have higher sensitivity in Hg(II) ion analysis than the UV-Vis spectrophotometry method and can detect Mercury ion concentrations down to the ppb level, it was used in this study [27]. In the digital image method, digital images captured with the Xiaomi X4 smartphone camera were used to determine the RGB Cys-AgNPs inten-

sity in Figure 10 in detecting Mercury ions (Hg(II)). Photoscape software, which separates the even colour concentration section from the standard solution (Cys-AgNPs + Mercury ions) and the blank digital image, was used to process the image.

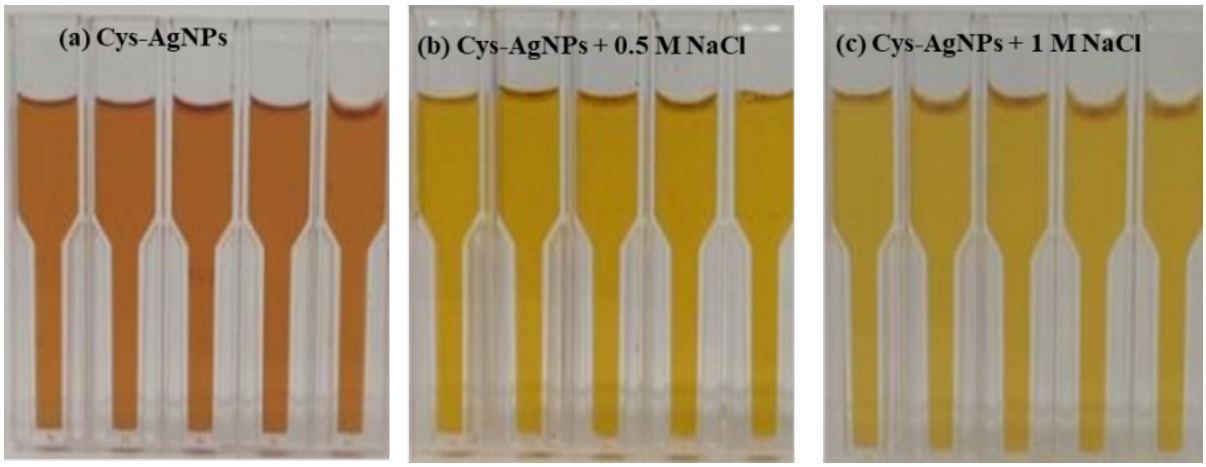

Figure 10. Visual Observation Results of Cys-AgNPs against Hg(II) solution (30-10ppb) for Making Digital Image Calibration Curves

Additionally, the value of each RGB colour component was obtained using the MATLAB R2010b program. The intensity of each colour component is assumed to be similar to the light intensity in the Lambert-Beer equation in spectrophotometry theory in order to determine the absorbance value of each colour component.

As shown in Figure 11, a calibration curve was created from the absorption value using the SLR (Simple Linear Regression) method for the digital image method. Digital images will be used to further process these RGB colour component values in the quantitative analysis of mercury ions. Moreover, RGB intensity is created from the RGB colour component values. The RGB intensity value can be obtained using the following Lamberts-Beer equation (Eq1). A calibration curve between RGB intensity and Hg ion concentration is then created using these RGB intensity data. Figure 11 displays the calibration curve for concentration versus RGB intensity. Because it has a larger slope than the G and R color components, Figure 11 demonstrates that the B (blue) color

component is the one that is most sensitive to changes. Additionally, its best linearity (R^2 = 0.9959) supports this. The reason for this is that the Cys-AgNPs have the highest absorbance in the blue component because they have a complementary colour that is near blue and a brownish-yellow colour.

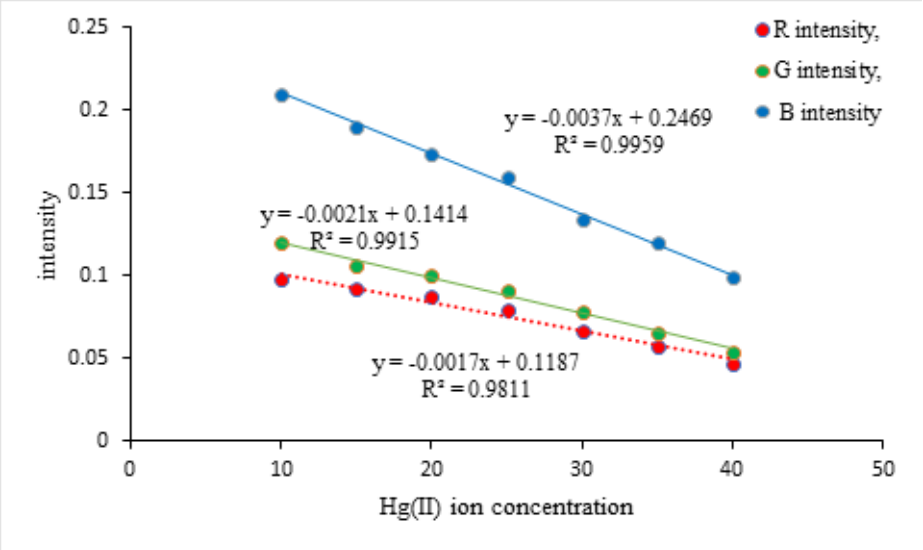

Figure 11. Calibration curve of digital image of Cys-AgNPs + Hg(II) solution (ppb)

Hg(II) ion analysis using the digital image method yielded Cys-AgNPs without the addition of NaCl, with a detection limit (LoD) of 5.79 ppb. Cys-AgNPs treated with 0.5 M and 1 m NaCl produced LoDs of 3.02 ppb and 2.46 ppb, respectively. Analysis of Hg(II) ions using the digital image method with the Cys-AgNPs indicator added with NaCl has been shown to detect mercury concentrations up to 5 ppb, the maximum mercury level allowed in the environment under the WHO limit [28].

In contrast, the described Hg (II) detection tests in real water samples revealed that the developed sensors support a limited hardness, so they were evaluated in tap water in the laboratory. It was discovered that the Cys-AgNPs-based sensor is more resistant to water hardness (calcium and magnesium content) than the AgNPs-Cy-based sensor because when the interferents were tested, the Cys-AgNPs sensor supported a higher concentration of

calcium, with the exception of magnesium, which it still responds to at low concentrations. On the other hand, both sensors perform well in detecting Hg (II) and small errors.

3.5 Expected mechanism in the current study

Sabela et al. (2017) [29] demonstrate how Cys-AgNPs interact with mercury via an aggregation mechanism, as shown in Figure 12, where chemisorption-type interactions result in AgNP aggregation via the carboxylate group of Cys with the Hg(II) ion, in a ratio of two Cy for each metal ion.

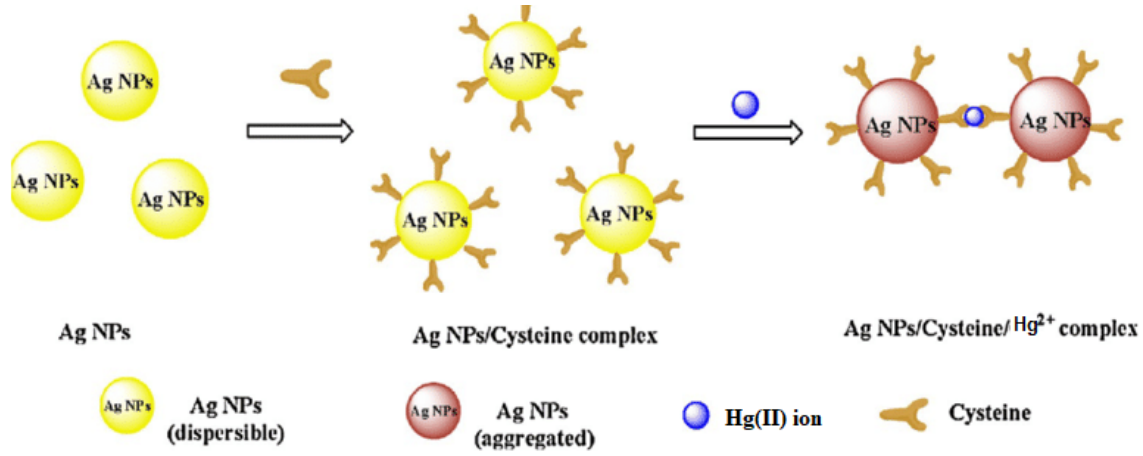

Figure 12: Schematic representation of the interaction between Cys-AgNPs and Hg(II) ion [29].

3.6 Comparison of Literature with the current work

Muhammed Abdel Hasan Shalla (2024) [31] evaluated silver nanoparticles (AgNPs) and AgNPs combined with cysteamine (Cy), with average diameters of 30±2 nm and 109 nm, respectively, for the detection of mercury (Hg(II)) in water at concentrations above 2 ppb. Mwakalesi et al. (2023) [32] developed a colorimetric sensor for detecting mercury in aqueous solutions using silver nanoparticles synthesized from an aqueous extract of *Synadenium glaucescens* root. These silver nanoparticles exhibited high selectivity for mercury, distinguishing it from other divalent metal ions. However, further research is needed to explore the practical applications of these silver nanoparticles (SYDR-AgNPs) in detecting mercury ions in real-world

samples.

Bhattacharjee et al. (2014) [33] developed cysteamine-stabilized silver nanoparticles in an aqueous medium, which were found to be highly sensitive and selective for rapid colorimetric detection of Hg(II) ions, with a detection limit (LOD) of 0.273 nM. Numerous detection methods [34-43] have been developed over the past decades, many of which employ complex and sophisticated techniques to detect Hg(II) ions at nanomolar to subnanomolar levels. In contrast, our simple, green, and economically viable technique achieves a detection limit of 5.79 ppb, which is comparable to or superior to many of the existing methods.

4. CONCLUSION

Stable nanoparticles with maximum LSPR absorbance in the spectrum of 402 nm and an average particle size of 65 nm were produced from *Sargassum boveanum* aqueous extract conjugated with 0.01 M L-cysteine. It has been demonstrated that adding NaCl solution raises the mercury ion detecting sensitivity of Cys-Silver Nanoparticles (Cys-AgNPs). NaCl added to Cys-AgNPs will be more sensitive to mercury ions the higher its concentration. Using digital images, the detection limit of Cys-AgNPs obtained from adding 0.5 M and 1 M NaCl solutions determines mercury ions at 3.02 and 2.46 ppb levels.

References

Baranwal, J., et al. "Electrochemical Sensors and Their Applications: A Review." *Chemosensors*, vol. 10, no. 9, 2022, p. 363.

Barhoum, Ahmed, et al. "Modern Designs of Electrochemical Sensor Platforms for Environmental Analyses: Principles, Nanofabrication Opportunities, and Challenges." *Trends in Environmental Analytical Chemistry*, vol. 38, 2023, e00199.

Hano, C., and B. H. Abbasi. "Plant-Based Green Synthesis of Nanoparticles: Production, Characterization and Applications." *Biomolecules*, 25 Dec. 2021, vol. 12, no. 1, p. 31.

Singh, H., et al. "Revisiting the Green Synthesis of Nanoparticles: Uncovering Influences of Plant Extracts as Reducing Agents for Enhanced Synthesis Efficiency and Its Biomedical Applications." *International Journal*

of Nanomedicine, vol. 18, 2023, pp. 4727-4750.

Al-Sulaiti, M. M., et al. "The Causes and Effects of Mercury and Methylmercury Contamination in the Marine Environment: A Review." *Current Pollution Reports*, vol. 8, no. 3, 2022, pp. 249-272.

Balali-Mood, M., et al. "Toxic Mechanisms of Five Heavy Metals: Mercury, Lead, Chromium, Cadmium, and Arsenic." *Frontiers in Pharmacology*, 13 Apr. 2021, vol. 12, p. 643972.

Sangaonkar, G. M., et al. "Selective Interaction between Phytomediated Anionic Silver Nanoparticles and Mercury Leading to Amalgam Formation Enables Highly Sensitive, Colourimetric and Memristor-Based Detection of Mercury." *Scientific Reports*, vol. 10, 2020, p. 2037.

Balasurya, S., et al. "Rapid Colourimetric Detection of Mercury Using Silver Nanoparticles in the Presence of Methionine." *Spectrochimica Acta Part A: Molecular and Biomolecular Spectroscopy*, vol. 228, 2020, p. 117712.

Sulistiawaty, Lilis, et al. "Detection of Hg2+ Metal Ions Using Silver Nanoparticles Stabilized by Gelatin and Tween-20." *Indonesian Journal of Chemistry*, vol. 15, 2015, pp. 1-8.

Alberti, G., et al. "Gold and Silver Nanoparticle-Based Colourimetric Sensors: New Trends and Applications." *Chemosensors*, vol. 9, no. 11, 2021, p. 305.

Yu, L., and N. Li. "Noble Metal Nanoparticles-Based Colourimetric Biosensor for Visual Quantification: A Mini Review." *Chemosensors*, vol. 7, no. 4, 2019, p. 53.

Borase, H. P., et al. "Mercury Sensing and Toxicity Studies of Novel Latex Fabricated Silver Nanoparticles." *Bioprocess and Biosystems Engineering*, vol. 37, 2014, pp. 2223-2233.

Osman, A. I., et al. "Synthesis of Green Nanoparticles for Energy, Biomedical, Environmental, Agricultural, and Food Applications: A Review." *Environmental Chemistry Letters*, vol. 22, 2024, pp. 841-887.

Guiry, M. D. "AlgaeBase." *National University of Ireland, Galway*, 15 Aug. 2012, https://www.algaebase.org. Accessed 6 Sept. 2024.

Mehdinezhad, N., A. Ghannadi, and A. Yegdaneh. "Phytochemical and Biological Evaluation of Some Sargassum Species from Persian Gulf." *Research*

in Pharmaceutical Sciences, vol. 11, no. 3, 2016, pp. 243-249.

Akbari, V., S. Zafari, and A. Yegdaneh. "Anti-Tuberculosis and Cytotoxic Evaluation of the Seaweed Sargassum Boveanum." *Research in Pharmaceutical Sciences*, vol. 13, no. 1, 2018, pp. 30-37.

González-Fuentes, F. J., et al. "Developing a CNT-SPE Sensing Platform Based on Green Synthesized AuNPs, Using Sargassum Sp." *Sensors*, vol. 20, no. 21, 2020, p. 6108.

Aktara, Mt, et al. "Synthesis of a Thiol Stabilized Silver Nanoparticle and Its Application towards Nanomolar Level Colourimetric Recognition of Glutathione." *New Journal of Chemistry*, vol. 43, 2019, p. 10.1039/C9NJ01360A.

Santos, J. P., L. Mehmeti, and V. I. Slaveykova. "Simple Acid Digestion Procedure for the Determination of Total Mercury in Plankton by Cold Vapor Atomic Fluorescence Spectroscopy." *Methods and Protocols*, vol. 5, no. 2, 2022, p. 29.

Hassan, S. A., and W. F. Hassan. "Structural and Spectral Studies of New Mixed Ligand Complexes for 2-Amino-4-Nitrophenol with Some Metallic Ions and Evaluation of Their Biological Activities." *Research Journal of Pharmacy and Technology*, vol. 15, no. 8, 2022, pp. 3634-3640.

Prosposito, P., et al. "Silver Nanoparticles as Colourimetric Sensors for Water Pollutants." *Chemosensors*, vol. 8, no. 2, 2020, p. 26.

Tewari, S., et al. "Green Synthesized AgNPs as a Probe for Colourimetric Detection of Hg (II) Ions in Aqueous Medium and Fluorescent Imaging in Liver Cell Lines and Its Antibacterial Activity." *Discover Nano*, vol. 19, 2024, p. 78.

Sanjeevappa, H. K., et al. "Biosynthesized Unmodified Silver Nanoparticles: A Colourimetric Optical Sensor for Detection of Hg2+ Ions in Aqueous Solution." *Results in Chemistry*, vol. 4, 2022, p. 100507.

Alwan, T. B., and S. A. Hassan. "Thermodynamic Studies of Cu (II) Complex of New Bidentate Schiff Base Ligand Type (NO) Derived from Mebendazol." *Egyptian Journal of Chemistry*, vol. 66, no. 1, 2023, pp. 563-572.

De Leersnyder, I., et al. "Revealing the Importance of Aging, Environment, Size and Stabilization Mechanisms on the Stability of Metal Nanoparticles:

A Case Study for Silver Nanoparticles in a Minimally Defined and Complex Undefined Bacterial Growth Medium." *Nanomaterials*, vol. 9, no. 12, 2019, p. 1684.

Hassan, S. A. "Synthesis and Characterization of Mixed Ligand Complexes from Curcumin and New Schiff Base Derived from Isatin for Some Metallic Ions and Evaluation Biological Activities." *Research Journal of Pharmacy and Technology*, vol. 15, no. 4, 2022, pp. 1537-1542.

Chen, K., et al. "Label-Free Colourimetric Detection of Mercury via Hg 2+ Ions-Accelerated Structural Transformation of Nanoscale Metal-Oxo Clusters." *Scientific Reports*, vol. 5, 2015, p. 16316.

Ebrahimi, S. J., A. Eslami, and L. Ebrahimzadeh. "Evaluation of Heavy Metals Concentration in the Drinking Water Distribution Network in Kurdistan Villages in the Year 2012." *Research Journal of Pharmaceutical, Biological and Chemical Sciences*, vol. 6, 2015, pp. 55-61.

Sabela, M. Y., et al. "A Review of Gold and Silver Nanoparticle-Based Colourimetric Sensing Assays." *Advanced Engineering Materials*, vol. 19, 2017, p. 1700270.

Naganthran A, Verasoundarapandian G, Khalid FE, Masarudin MJ, Zulkharnain A, Nawawi NM, Karim M, Che Abdullah CA, Ahmad SA. Synthesis, Characterization and Biomedical Application of Silver Nanoparticles. *Materials*. 15(2), 2022, p.:427

Shallal, Muhammed Abdel Hasan. "Evaluation of Silver Nanoparticles Stabilized with Sulfurized Ligands as Mercury (Hg II) Sensors in Water Samples." *Innovative: International Multidisciplinary Journal of Applied Technology*, vol. 2, no. 11, 2024, pp. 93-107.

Mwakalesi, A. J., and M. J. Nyangi. "Colorimetric Sensing of Mercury in Aqueous Solutions Using Silver Nanoparticles Prepared from *Synadenium glaucescens* Root Aqueous Extract." *Engineering Proceedings*, vol. 56, no. 1, 2023, p. 182, https://doi.org/10.3390/ASEC2023-15310.

Bhattacharjee, Yudhajit, and Amarnath Chakraborty. "Label-Free Cysteamine-Capped Silver Nanoparticle-Based Colorimetric Assay for Hg(II) Detection in Water with Subnanomolar Exactitude." *ACS Sustainable Chemistry & Engineering*, vol.

2, 2014, pp. 2149-2154, https://doi.org/10.1021/sc500339n.

Deng, L., Ouyang, X., Jin, J., Ma, C., Jiang, Y., Zheng, J., Li, J., Li, Y., Tan, W., and Yang, R. "Exploiting the Higher Specificity of Silver Amalgamation: Selective Detection of Mercury(II) by Forming Ag/Hg Amalgam." *Analytical Chemistry*, vol. 85, no. 18, 2013, pp. 8594-8600.

Schiesaro, Irene, et al. "Hydrophilic Silver Nanoparticles for Hg(II) Detection in Water: Direct Evidence for Mercury–Silver Interaction." *The Journal of Physical Chemistry C*, vol. 124, no. 47, 2020, pp. 25975-25983, https://doi.org/10.1021/acs.jpcc.0c06951.

Vyas, Gaurav, Shreya Bhatt, and Parimal Paul. "Synthesis of Calixarene-Capped Silver Nanoparticles for Colorimetric and Amperometric Detection of Mercury (HgII, Hg0)." *ACS Omega*, vol. 4, no. 2, 2019, pp. 3860-3870, https://doi.org/10.1021/acsomega.8b03299.

Wen, Shao-Hua, Ru-Ping Liang, Li Zhang, and Jian-Ding Qiu. "Multimodal Assay of Arsenite Contamination in Environmental Samples with Improved Sensitivity through Stimuli-Response of Multiligands Modified Silver Nanoparticles." *ACS Sustainable Chemistry & Engineering*, vol. 6, no. 5, 2018, pp. 6223-6232, https://doi.org/10.1021/acssuschemeng.7b04934.

Kim, Dae-Young, et al. "Alginic Acid-Functionalized Silver Nanoparticles: A Rapid Monitoring Tool for Detecting the Technology-Critical Element Tellurium." *Journal of Hazardous Materials*, vol. 465, 2024, 133161, https://doi.org/10.1016/j.jhazmat.2023.133161.

Anitha, R., and G. R. Rajarajeswari. "Selective and Ultrasensitive Spectroscopic Detection of Mercuric Ion in Aqueous Systems Using Embonic Acid Functionalized Silver Nanoparticle." *Journal of Cluster Science*, vol. 34, no. 4, 2023, pp. 1999-2015, https://doi.org/10.1007/s10876-022-02366-8.

Hai, Nguyen Duy, et al. "Phytosynthesis of Silver Nanoparticles Using *Mangifera indica* Leaves Extract at Room Temperature: Formation Mechanism, Catalytic Reduction, Colorimetric Sensing, and Antimicrobial Activity." *Colloids and Surfaces B: Biointerfaces*, vol. 220, 2022, 112974, https://doi.org/10.1016/j.colsurfb.2022.112974.

Rajkumar, Ganesan, and Rajara-

man Sundar. "Sonochemical-Assisted Eco-Friendly Synthesis of Silver Nanoparticles (AgNPs) Using Avocado Seed Extract: Naked-Eye Selective Colorimetric Recognition of Hg2+ Ions in Aqueous Medium." *Journal of Molecular Liquids*, vol. 368, 2022, 120638, https://doi.org/10.1016/j.molliq.2022.120638.

Kumar, Pradeep, et al. "Sensing of Mercury Ion Using Light Induced Aqueous Leaf Extract Mediated Green Synthesized Silver Nanoparticles of *Cestrum nocturnum* L." *Environmental Science and Pollution Research*, vol. 29, no. 53, 2022, pp. 79995-80004, https://doi.org/10.1007/s11356-022-19357-x.

Huang, Jinkun, et al. "Tyndall-Effect-Enhanced Supersensitive Naked-Eye Determination of Mercury (II) Ions with Silver Nanoparticles." *Sensors and Actuators B: Chemical*, vol. 344, 2021, 130218, https://doi.org/10.1016/j.snb.2021.130218.